Spectral information and distinguishability in type-II down-conversion with a broadband pump

W. P. Grice and I. A. Walmsley
The Institute of Optics, University of Rochester, Rochester, New York 14627
(Received 30 August 1996; revised manuscript received 28 March 1997)

A model is presented to describe spontaneous type-II parametric down-conversion pumped by a broadband source. This process differs from the familiar cw-pumped down-conversion in that a broader range of pump energies is available for down-conversion. The properties of the nonlinear crystal determine how these energies are distributed into the down-converted photons. Because the two photons are polarized along different crystal axes, they have different spectral characteristics and are no longer exactly anticorrelated. As the pump bandwidth is increased, this effect becomes more pronounced. A fourth-order interference experiment is proposed, illustrating some of the features of broadband pumped down-conversion. [S1050-2947(97)08508-9]

PACS number(s): 42.50.Dv, 03.65.Bz, 42.65.Ky

I. INTRODUCTION

Pairs of particles with a high degree of correlation exhibit behavior that exposes many interesting features of quantum mechanics. A common method for generating highly correlated photon pairs is spontaneous parametric down-conversion pumped by a single-frequency laser. In this process, the coherence times of the down-converted photons are determined entirely by the crystal parameters and can be quite short [1]. As a result, the photon wave packets are well localized with respect to one another. In addition, energy conservation ensures that the frequencies of the down-converted photons always sum to the pump frequency. The photons are correlated in position and anticorrelated in energy in the sense that a measurement of either of these parameters in one photon yields knowledge of the corresponding parameter in the second. Several experimentalists have used this type of process to produce entangled states in order to demonstrate violations of Bell's inequalities [2–4]. Another series of experiments, employing a Hong-Ou-Mandel interferometer, has been carried out to investigate the role of distinguishability in interference [1,5,6]. In most of these experiments, the down-converter is simply used as a convenient source of correlated photons and the interesting physics takes place through their subsequent manipulation. A couple of recent works, though, investigate the down-conversion process in more detail by varying different pump parameters. Specifically, the spatial distribution of the down-converted photon pairs is studied in the context of variable pump spectral width [7] and wave-front curvature [8].

While the emission times of the two photons produced in cw-pumped down-conversion are well known with respect to one another, the absolute time of emission is completely random. The reason, of course, is that the process is pumped with a cw source, which has an essentially infinite coherence length. One way to remove some of the uncertainty in the emission time is to use a pulsed laser to pump the crystal. Clearly, this type of approach is necessary for experiments in which separate crystals are required to emit at nearly simultaneous times [9–11]. Similar methods have been suggested as a means of realizing the experiment proposed by Greenberger, Horne, and Zeilinger [12–15]. An implicit assumption in many of these proposals is that the photons generated from different crystals are synchronized to within their coherence times. This might be accomplished by decreasing the emission time window by using shorter pulses to pump the process. But when the down-conversion process is pumped with a broadband source, the coherence times of the down-converted photons are affected not only by the crystal parameters, but also by the coherence time of the pump. In addition, the energy constraint is relaxed because a broad range of frequencies is present in the pump pulse. Consequently, the frequencies of the down-converted photons are no longer exactly anticorrelated. It is clear that a better understanding of broadband-pumped down-conversion is needed in order to analyze the above proposals.

In this paper, we consider spontaneous parametric down-conversion pumped by a broadband source. We restrict ourselves to the case in which the down-converted beams are collinear with the pump. The motivation for this choice is related to the broadband nature of the pump. Conservation of momentum ensures that the propagation directions of the down-converted photons are correlated. But since there is a broad range of k vectors in the pump, a given propagation direction for one photon corresponds to a range of directions for the other. The exception is the case in which the two photons have no transverse momentum components, i.e., when they are collinear with the pump. We also restrict our analysis to type-II down-conversion, in which the down-converted photons have orthogonal polarizations. This is more practical for experiments in which the two photons are to be manipulated independently. In Sec. II, we present a model describing the two-photon state produced by pulsed type-II spontaneous down-conversion. We find that, in contrast to cw-pumped down-conversion, the two photons produced in pulsed type-II down-conversion have different spectra. This difference becomes more pronounced as the pump bandwidth is increased. In Sec. III, we analyze a proposed experiment in which the additional information carried by the photons causes a reduction of visibility in fourth-order interference. Section IV contains discussion and conclusions.

II. TWO-PHOTON STATE

The process of parametric down-conversion can be studied in the interaction picture, in which the evolution of the state vector is given by

$$|\psi(t)\rangle = \exp\left[\frac{1}{i\hbar}\int_{t_0}^{t} dt' \hat{H}_I(t')\right]|\psi_0\rangle, \tag{1}$$

where $|\psi_0\rangle$ is the state at time t_0 and $\hat{H}_I(t)$ is the interaction Hamiltonian. For type-II down-conversion, this Hamiltonian may be taken to be

$$\hat{H}_I(t) = \int_{\nu} d^3r \chi^{(2)} \hat{E}_p^{(+)}(\mathbf{r},t)\hat{E}_o^{(-)}(\mathbf{r},t)\hat{E}_e^{(-)}(\mathbf{r},t) + \text{H.c.}, \tag{2}$$

where V is the volume of the nonlinear crystal and $\hat{E}_j(\mathbf{r},t) = \hat{E}_j^{(+)}(\mathbf{r},t) + \hat{E}_j^{(-)}(\mathbf{r},t)$ are the three interacting fields. Here $j = p,o,e$ identifies the pump, ordinary, and extraordinary waves, respectively. The crystal's nonlinearity is characterized by $\chi^{(2)}$, which is assumed to be independent of frequency over the region of interest. This assumption dismisses higher-order effects of dispersion, which can become important in some ultrafast applications. As will be seen later, the assumption is warranted in this case because the interaction is governed by the phase-matching conditions, which arise from the dispersion in $\chi^{(1)}$. This effect is much more significant than those arising from a dispersive $\chi^{(2)}$.

To simplify the analysis, the down-converted beams are constrained to be collinear with the pump beam. In practice, this can be achieved through the use of pinholes. The volume integral in Eq. (2) then becomes an integral over only one direction, say z. The positive frequency part of $\hat{E}_j(z,t)$ is

$$\hat{E}_j^{(+)}(z,t) = \int d\omega_j A(\omega_j)\hat{a}_j(\omega_j)e^{i[k_j(\omega_j)z - \omega_j t]}, \tag{3}$$

where $\hat{a}_j(\omega_j)$ is the photon annihilation operator for the mode defined by frequency ω_j, the z direction, and the polarization associated with the index j. $A(\omega_j) = i\sqrt{\hbar\omega_j/2\epsilon_0 n^2(\omega_j)}$ is a slowly varying function of frequency and may be taken outside the integral. $\hat{E}_j^{(-)}(z,t)$ is related to $\hat{E}_j^{(+)}(z,t)$ by $\hat{E}_j^{(-)}(z,t) = [\hat{E}_j^{(+)}(z,t)]^{\dagger}$. Since spontaneous parametric down-conversion is a very inefficient process, the pump field must be relatively large. Accordingly, the electric-field operator $\hat{E}_p^{(+)}(\mathbf{r},t)$ may be replaced by the classical field $E_p(\mathbf{r},t) = \tilde{\alpha}(t)e^{ik_p(\omega_p)z}$ [16]. The interaction Hamiltonian may now be expressed as

$$\hat{H}_I(t) = A\int_{-L/2}^{L/2} dz \int d\omega_0 \int d\omega_e \hat{a}_o^{\dagger}(\omega_o)\hat{a}_e^{\dagger}(\omega_e)\tilde{\alpha}(t) \times e^{-i\{[k_o(\omega_o)+k_e(\omega_e)-k_p(\omega_p)]z-[\omega_o+\omega_e]t\}} + \text{H.c.}, \tag{4}$$

where L is the length of the crystal and $A(\omega_j)$ has been grouped into the parameter A, along with several constants.

The time-dependent part of the interaction Hamiltonian is $\tilde{\alpha}(t)e^{i(\omega_o+\omega_e)t}$, which goes to zero whenever the pump field goes to zero. If the process is pumped by a pulsed laser, then the interaction is nonzero for only a short period of time. The interaction time is essentially determined by the pulse duration. It is assumed that at time t_0 the pump field is zero inside the crystal and that the pulse enters the crystal some time later. We restrict our attention to times t after the completion of the interaction, i.e., after the pulse has exited the crystal. Thus, the interaction Hamiltonian is zero for times before t_0 or after t. The limits of integration in Eq. (1) may therefore be extended to infinity. It has been shown with a more general argument that these limits of integration may be extended to infinity even if the pump field is not in the form of a coherent pulse [17]. With the revised limits of integration, the integral is somewhat easier to handle if the pump field is represented as a Fourier decomposition. The integral in Eq. (1) then becomes

$$\int_{t_0}^{t} dt' \hat{H}_I(t') = A\int_{-\infty}^{\infty} dt' \int_{-L/2}^{L/2} dz \int d\omega_o \times \int d\omega_e \hat{a}_o^{\dagger}(\omega_o)\hat{a}_e^{\dagger}(\omega_e)\int d\omega_p \alpha(\omega_p) \times e^{-i\{[k_o(\omega_o)+k_e(\omega_e)-k_p(\omega_p)]z-[\omega_o+\omega_e-\omega_p]t\}} + \text{H.c.}, \tag{5}$$

where $\alpha(\omega)$ is the Fourier transform of $\tilde{\alpha}(t)$. The time integral is performed first, yielding $2\pi\delta(\omega_o+\omega_e-\omega_p)$. Evaluating one of the frequency integrals gives

$$\int_{t_0}^{t} dt' \hat{H}_I(t') = 2\pi A\int_{-L/2}^{L/2} dz \int d\omega_o \int d\omega_e \hat{a}_o^{\dagger}(\omega_o) \times \hat{a}_e^{\dagger}(\omega_e)\alpha(\omega_o+\omega_e) \times e^{-i[k_o(\omega_o)+k_e(\omega_e)-k_p(\omega_o+\omega_e)]z} + \text{H.c.} \tag{6}$$

The integration over the length of the crystal is easily performed, giving

$$\int_{t_0}^{t} dt' \hat{H}_I(t') = 2\pi A\int d\omega_o \int d\omega_e \hat{a}_o^{\dagger}(\omega_o)\hat{a}_e^{\dagger}(\omega_e) \times \alpha(\omega_o+\omega_e)\Phi(\omega_o,\omega_e) + \text{H.c.}, \tag{7}$$

where

$$\Phi(\omega_o,\omega_e) = \frac{\sin\{[k_o(\omega_o)+k_e(\omega_e)-k_p(\omega_o+\omega_e)]L\}}{[k_o(\omega_o)+k_e(\omega_e)-k_p(\omega_o+\omega_e)]L}. \tag{8}$$

Since the interaction is fairly weak, the unitary time evolution operator in Eq. (1) may be approximated by the first two terms of a perturbative expansion. The first term is simply the initial state, which is assumed to be the vacuum state. The term of interest is the second term, which is

$$|\psi_2\rangle = \frac{2\pi A}{i\hbar}\int d\omega_o \int d\omega_e \alpha(\omega_o+\omega_e) \times \Phi(\omega_o,\omega_e)|\omega_o\rangle_o|\omega_e\rangle_e, \tag{9}$$

where $|\omega_i\rangle_j$ is a one-photon Fock state. Equation (9) represents a superposition of two-photon states in which the o-polarized photon has frequency ω_o and the e-polarized photon has frequency ω_e. The probability amplitude associated with each pair is the product of the pump envelope function $\alpha(\omega_o+\omega_e)$ and the phase-matching function

$\Phi(\omega_o,\omega_e)$. The pump envelope function ensures conservation of energy. That is, a down-conversion event is allowed only if the energies of the daughter photons sum to some frequency found in the pump. For a given pump photon, the phase-matching function determines how the energy is to be distributed. Since the pump envelope function depends on the sum frequency, it is symmetric with respect to ω_0 and ω_e. It can be seen from Eq. (8), however, that this is not the case for the phase-matching function $\Phi(\omega_0,\omega_e)$. Because the crystal is birefringent, $k_o(\omega)\neq k_e(\omega)$ in general and $\Phi(\omega_o,\omega_e)$ is not symmetric in its frequency arguments. That is, $\Phi(\omega_o,\omega_e)\neq\Phi(\omega_e,\omega_o)$. Because of this asymmetry, the wave packets describing the two photons produced in pulsed type-II down-conversion are not identical, even when they are degenerate in their center frequencies.

The essential character of the phase-matching function is better illustrated when it is expressed in a simpler form obtained by making the Taylor expansions $k_p(\omega)=k_{p0}+(\omega-2\overline{\omega})k_p'+\cdots$ and $k_j(\omega)=k_{j0}+(\omega-\overline{\omega})k_j'+\cdots$ $(j=o,e)$, where $k_{p0}=k_p(2\overline{\omega})$, $k_{j0}=k_j(\overline{\omega})$, $k_p'=\partial k_p(\omega)/\partial\omega|_{\omega=2\overline{\omega}}$, and $k_j'=\partial k_j(\omega)/\partial\omega|_{\omega=\overline{\omega}}$. Here, $2\overline{\omega}$ is the center pump frequency. Discarding all but the first two terms yields

$$k_o(\omega_o)+k_e(\omega_e)-k_p(\omega_o+\omega_e)\cong\nu_o(k_o'-k_p')+\nu_e(k_e'-k_p'), \tag{10}$$

where $\nu_j=\omega_j-\overline{\omega}$ $(j=o,e)$ are the difference frequencies and perfect phase matching at the center frequencies gives $k_{o0}+k_{e0}-k_{p0}=0$. Using Eq. (10), the phase-matching function becomes

$$\Phi(\overline{\omega}+\nu_o,\overline{\omega}+\nu_e)=\frac{\sin\{[\nu_o(k_o'-k_p')+\nu_e(k_e'-k_p')]L\}}{[\nu_o(k_o'-k_p')+\nu_e(k_e'-k_p')]L}. \tag{11}$$

Figure 1(a) shows a plot of $|\Phi(\overline{\omega}+\nu_o,\overline{\omega}+\nu_e)|^2$ for typical values of k_o', k_e', and k_p'. In this plot (and in all subsequent plots), the difference frequencies have been normalized by $\Delta\nu_{\rm cw}=2.78/|k_o'-k_e'|L$, the bandwidth found in type-II parametric down-conversion pumped by a cw source. The phase-matching function attains its maximum value whenever $\nu_o(k_o'-k_p')=-\nu_e(k_e'-k_p')$ and has constant value along any contour parallel to the line defined by this relation. This distribution determines how the energy in a given pump photon is distributed to the two down-converted photons. The *range* of pump frequencies available for down-conversion is determined by the pump envelope function $\alpha(\omega_o+\omega_e)$. Since this function depends on $\omega_o+\omega_e=2\overline{\omega}+\nu_o+\nu_e$, its contour lines are parallel to the line defined by $\nu_o=-\nu_e$. Figure 1(b) shows a plot of $|\alpha(2\overline{\omega}+\nu_o+\nu_e)\Phi(\overline{\omega}+\nu_o,\overline{\omega}+\nu_e)|^2$, where a Gaussian shape has been assumed for the pump envelope.

It is useful to think of this plot as the probability distribution for the two-photon state. That is, the probability that the o-polarized photon has frequency $\omega_o=\overline{\omega}+\nu_o$ and the e-polarized photon has frequency $\omega_e=\overline{\omega}+\nu_e$ is proportional to the value of the function at the point (ν_o,ν_e). This plot also demonstrates a feature that is important in the experiment described below. As the pump bandwidth is increased, the overlap between the pump envelope and the phase-matching function also increases. More pump frequencies are available for down-conversion, and a larger range of frequencies are found in both down-converted beams, but the

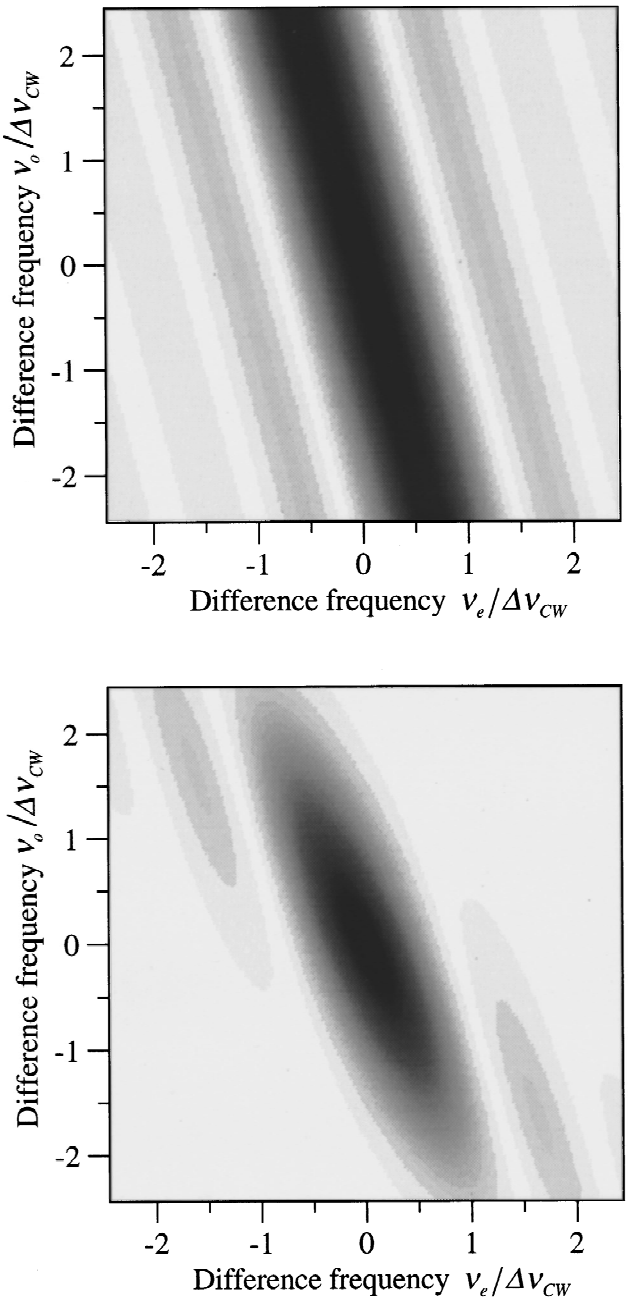

FIG. 1. Plot of the phase-matching function alone (a) and multiplied by the pump envelope function (b). The axes are the difference frequencies for the o- and e-polarized photon wave packets. The difference frequencies are normalized by the characteristic frequency $\Delta\nu_{\rm cw}$.

asymmetry of the phase-matching function causes one of the down-converted spectra to grow more quickly than the other. The spectra $S_o(\nu)$ and $S_e(\nu)$ of the individual photon wave packets are

$$S_o(\nu)=\int d\nu_e|\alpha(2\overline{\omega}+\nu+\nu_e)\Phi(\overline{\omega}+\nu,\overline{\omega}+\nu_e)|^2,$$

$$S_e(\nu)=\int d\nu_o|\alpha(2\overline{\omega}+\nu+\nu_o)\Phi(\overline{\omega}+\nu_o,\overline{\omega}+\nu)|^2. \tag{12}$$

That is, the difference frequency spectrum of the o-polarized (e-polarized) photon wave packet is found by

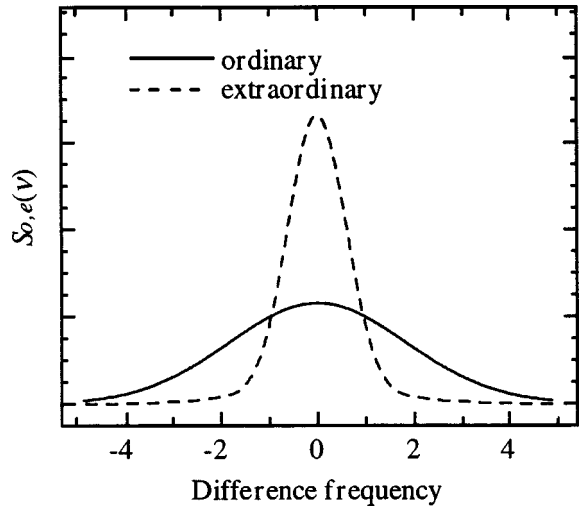

FIG. 2. Spectra of the o- and e-polarized photon wave packets for the distribution shown in Fig. 1(b). Again, the difference frequency is normalized by $\Delta\nu_{\mathrm{cw}}$.

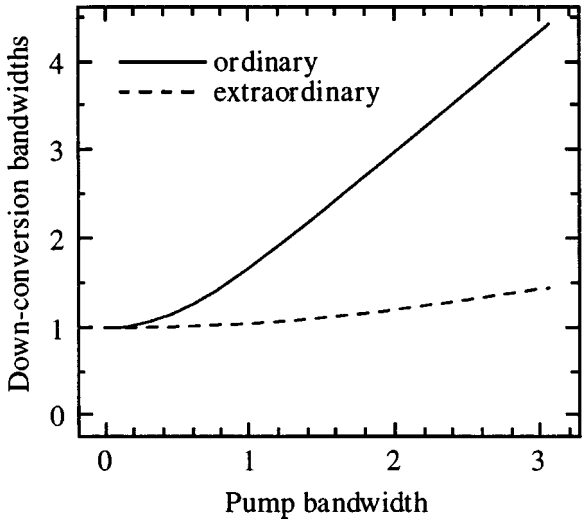

FIG. 3. Bandwidths of the o- and e-polarized photon wave packets plotted as a function of the pump bandwidth. All values are normalized by $\Delta\nu_{\mathrm{cw}}$.

projecting $|\alpha(2\overline{\omega}+\nu_o+\nu_e)\Phi(\overline{\omega}+\nu_o,\overline{\omega}+\nu_e)|^2$ onto the ν_o (ν_e) axis. Figure 2 shows the two spectra for the distribution of Fig. 1(b). As expected, the spectrum of the o-polarized photon wave packet is broader than that of the e-polarized photon. The bandwidths of the two down-converted fields have been calculated for several different values of the pump bandwidth. The results are plotted in Fig. 3 as a function of pump bandwidth, which is also normalized by $\Delta\nu_{\mathrm{cw}}$.

It should be noted that if a cw pump with frequency $2\overline{\omega}$ is used, then the pump envelope function becomes a delta function $\delta(\omega_o+\omega_e-2\overline{\omega})$ and Eq. (9) reduces to the familiar expression for cw-pumped down-conversion [18],

$$|\psi_2\rangle_{\mathrm{cw}}=\frac{2\pi A}{i\hbar}\int d\omega\ \Phi(\overline{\omega}+\nu,\overline{\omega}-\nu)|\overline{\omega}+\nu\rangle_o|\overline{\omega}-\nu\rangle_e. \tag{13}$$

There are several important differences between states described by Eqs. (9) and (13). First, the two beams produced in cw-pumped down-conversion are exactly anticorrelated in frequency, because energy conservation requires that the down-converted frequencies always sum to the pump frequency, $2\overline{\omega}$. Of course, it is still true that energy is conserved in broadband-pumped down-conversion, but instead of a single pump frequency, there is a broad range of frequencies available. As a consequence, the down-converted frequencies no longer sum to a constant value. They are no longer exactly anticorrelated. The second difference concerns the symmetry of the frequency distributions. With a broadband pump, the asymmetry of the phase-matching function leads to down-converted photon wave packets with spectra that can be quite different. This is not the case in the cw limit. Since the frequencies are exactly anticorrelated, the two-photon state represented by Eq. (13) is symmetric in the two frequencies. Therefore, the spectra of the e- and o-polarized photon wave packets are identical. Indeed, Fig. 3 shows that the two photons have the same bandwidth as the pump bandwidth approaches zero.

Another difference between the two states involves the temporal characteristics of the down-converted fields. Two quantities are of interest: the coherence times and the time of emission. Just as with a broadband pump, the photons produced in cw-pumped down-conversion can have large bandwidths and, consequently, short coherence times. The two states are similar in that this quantity is determined by the interplay of the phase-matching function and the pump envelope function. But regarding the time of emission, the two cases are quite different. For a cw pump, the time of emission is completely random. That is, the down-conversion probability is independent of time. This is obviously not the case for a pulsed pump field, since a down-conversion event can only occur when the pulse passes through the crystal. Thus a pulsed pump field leads to a reduced uncertainty in the time of emission as compared to a cw pump. It should be pointed out that for experiments involving photons from a single down-conversion source, the absolute time of emission is not relevant, but in the case of multiple sources one requires that the time of emission of the photons have a smaller variance than their coherence time.

III. A PROPOSED EXPERIMENT

Many experiments involving cw-pumped down-conversion have exploited the fact that the two output photons have identical spectral characteristics. In particular, when the photons are mixed in a Hong-Ou-Mandel interferometer, their indistinguishability leads to a fourth-order interference effect [1,5,6], but when the photons originate in a type-II crystal pumped by a broadband source, the visibility of the interference is decreased. The reason for this is that, since the two photons have different spectral characteristics, they carry information about the two interfering paths. The amount of information increases as the pump bandwidth is increased. The visibility of the fourth-order interference can be restored, however, by selecting only those runs for which the two paths are indistinguishable.

The experimental apparatus, shown schematically in Fig. 4, is similar to that used by other experimentalists to investigate fourth-order interference in type-II down-conversion [6,19,20]. The primary difference here is that a broadband pump with variable bandwidth is used to pump the down-

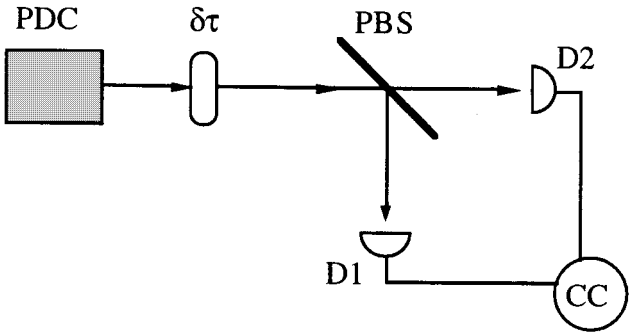

FIG. 4. Layout of the proposed experiment. The parametric down-converter (PDC) is pumped by a variable bandwidth source. The o- and e-polarized photons travel collinearly to the polarization beam splitter (PBS), which is oriented at 45° with respect to polarization axes. Coincidence counts are measured at detectors $D1$ and $D2$ as a function of the relative delay $\delta\tau$. This delay can be adjusted by adding or removing birefringent material from the beam path.

conversion process. The o- and e-polarized photons then travel collinearly and are mixed at a polarization beam splitter oriented at 45° with respect to the two polarizations. The outputs of the beam splitter are directed to detectors $D1$ and $D2$, and the coincidence rate is measured as a function of the relative delay between the two polarizations. This delay can be realized by inserting an appropriate amount of birefringent material before the polarization beam splitter.

Suppressing the z dependence, the field operators at the detectors $D1$ and $D2$ are given by

$$\hat{E}_1^{(+)}(t)=\frac{1}{\sqrt{2}}[\hat{E}_o^{(+)}(t)+\hat{E}_e^{(+)}(t+\delta\tau)],$$

$$\hat{E}_2^{(+)}(t)=\frac{1}{\sqrt{2}}[\hat{E}_o^{(+)}(t)-\hat{E}_e^{(+)}(t+\delta\tau)], \tag{14}$$

where $\delta\tau$ is the relative delay between the two photons and

$$\hat{E}_{o,e}^{(+)}(t)\propto\int d\nu\ \hat{a}_{o,e}(\overline{\omega}+\nu)e^{-i(\overline{\omega}+\nu)t}. \tag{15}$$

The probability of detecting one photon at detector $D1$ at time t_1 and one photon at detector $D2$ at time t_2 is

$$P_{12}(t_1,t_2;\delta\tau)=\langle\hat{E}_1^{(-)}(t_1)\hat{E}_2^{(-)}(t_2)\hat{E}_2^{(+)}(t_2)\hat{E}_1^{(+)}(t_1)\rangle. \tag{16}$$

Using Eq. (9) for the state and Eqs. (14) and (15) for the field operators, this expression becomes

$$P_{12}(t_1,t_2;\delta\tau)\propto\left|\int\int d\omega_o d\omega_e\alpha(\omega_o+\omega_e)\times\Phi(\omega_o,\omega_e)e^{-i\omega_e\delta\tau}[e^{-i(\omega_o t_2+\omega_e t_1)}-e^{-i(\omega_o t_1+\omega_e t_2)}]\right|^2. \tag{17}$$

The average coincidence counting rate is given by

$$R_c(\delta\tau)=\frac{1}{T}\int\int_0^T dt_1 dt_2 P_{12}(t_1,t_2;\delta\tau), \tag{18}$$

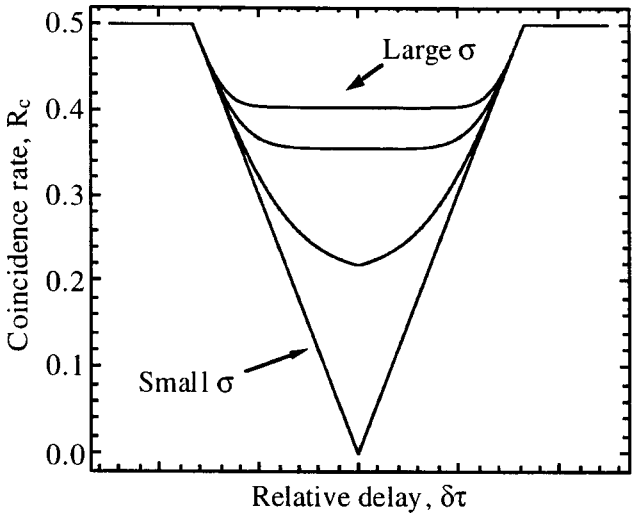

FIG. 5. The coincidence rate plotted as a function of relative delay between the down-converted photons. The delay is normalized by $1/\Delta\nu_{\rm cm}$, the inverse of the characteristic bandwidth. The different curves represent the coincidence rate for different values of the pump bandwidth. The curve labeled ''Small σ'' corresponds to a cw pump, while ''Large σ'' corresponds to a pump bandwidth 3 times larger than the characteristic bandwidth $\Delta\nu_{\rm cw}$.

where T is the coincidence detection time, typically on the order of a few nanoseconds. Because T is much longer than the interaction time, the limits of integration may be extended to infinity, giving

$$R_c(\delta\tau)\propto\int\int d\omega_o d\omega_e|\alpha(\omega_o+\omega_e)|^2[|\Phi(\omega_o,\omega_e)|^2-\Phi(\omega_o,\omega_e)\Phi^*(\omega_e,\omega_o)e^{-i(\omega_e-\omega_o)\delta\tau}]. \tag{19}$$

The first term in this expression represents an integration over the entire two-photon probability distribution. It is proportional to the total probability of observing a down-conversion event, regardless of the frequencies of the down-converted photons. When $\delta\tau$ is large, the second term oscillates rapidly as a function of frequency and contributes nothing to the integral, leaving only the first term to establish the background level. As $\delta\tau$ approaches zero, the second term contributes and the coincidence rate falls. When $\delta\tau=0$ exactly, the only difference between the two terms is that the arguments of Φ^* are reversed in the second term. This subtle change has an important consequence, though. Since Φ is not symmetric in its frequency arguments, $\Phi(\omega_o,\omega_e)$ and $\Phi^*(\omega_e,\omega_o)$ overlap only when $\omega_o\approx\omega_e$. This is the case when the pump spectrum is narrow. In the cw-pump limit, in fact, the phase-matching function is symmetric in its frequency arguments and the coincidence rate goes to zero for $\delta\tau=0$. As the pump spectrum is increased, the pump envelope $\alpha(\omega_o+\omega_e)$ grows to include contributions from the regions of the distribution for which ω_o and ω_e are very different. While the amplitude of $\Phi(\omega_o,\omega_e)\Phi^*(\omega_e,\omega_o)$ is very small in these regions, Fig. 1(a) shows that $|\Phi(\omega_o,\omega_e)|^2$ has significant value for all pump frequencies. The result is that the first term becomes much larger than the second and the coincidence rate no longer goes to zero.

Equation (19) can be integrated to give

$$R_c(\delta\tau) \propto \begin{cases} \dfrac{1}{\sqrt{2\pi}}\dfrac{\sigma}{\Omega_+} - \mathrm{erf}\left[\dfrac{1}{2\sqrt{2}}\dfrac{\sigma}{\Omega_+}(1-|\delta\tau|\Omega_-)\right], & |\delta\tau| < \dfrac{1}{\Omega_-} \\ \dfrac{1}{\sqrt{2\pi}}\dfrac{\sigma}{\Omega_+}, & \text{otherwise,} \end{cases} \tag{20}$$

where $1/\Omega_\pm = L|(k_p' - k_e') \pm (k_p' - k_o')|$ and σ is proportional to the pump bandwidth. As before, the pump spectrum is assumed to have a Gaussian shape. Figure 5 contains normalized plots of $R_c(\delta\tau)$ for several values of the pump bandwidth. In the cw-pump limit, $\sigma \to 0$ and the function has the familiar triangle shape [6]. As the pump bandwidth increases, the depth of the dip decreases. In the limit of infinite pump bandwidth, in fact, the dip disappears entirely.

The diminished visibility in the fourth-order interference can be attributed to increased distinguishability of the two photons. More correctly, it is caused by the distinguishability of the two paths leading to coincidence counts. A coincidence count can occur *either* when the *o*-polarized photon is detected at detector $D1$ and the *e*-polarized photon is detected at detector $D2$ *or* when the *e*-polarized photon is detected at detector $D1$ and the *o*-polarized photon is detected at detector $D2$. When it is impossible to distinguish between these two processes, destructive interference causes the count rate to fall to zero. With a large pump bandwidth, the two photons have different spectra, making the two paths somewhat distinguishable. In addition, certain combinations of the downconverted frequencies ω_o and ω_e are more likely than others. By measuring the energies of the detected photons, it would be possible in many cases to determine the path taken by each. For example, measuring frequencies ω_1 and ω_2 at detectors $D1$ and $D2$, respectively, would imply that *either* $\omega_1 = \omega_o$ and $\omega_2 = \omega_e$ or $\omega_1 = \omega_e$ and $\omega_2 = \omega_o$. Each of the possible outcomes has an associated probability amplitude. The geometry of the interferometer is such that these two amplitudes have opposite signs and they therefore sum to zero when their magnitudes are equal. But because $\Phi(\omega_o, \omega_e) \neq \Phi(\omega_e, \omega_o)$, this is not the case for most frequency pairs. Of course, one does not actually have to measure the energies of the detected photons in order to destroy the interference. It is sufficient that this measurement is possible in principle.

It is interesting to note that, as long as the pump bandwidth is not infinite, the interference cannot be completely destroyed. That is, the visibility never quite reaches zero. The reason for this is that, in many cases, the photons have similar energies and it is difficult to gain information about the paths taken by the two photons. These ''indistinguishable'' runs are always present, even for a large pump bandwidth. A broader pump spectrum simply facilitates a larger proportion of ''distinguishable'' down-conversions, i.e., a larger proportion of runs in which the energies of the down-converted photons are significantly different. If a measurement of the coincidence counting rate were performed only on the indistinguishable runs, then the interference would be restored. This could be accomplished by placing spectral filters in front of the detectors. To demonstrate this feature, numerical calculations were carried out to determine the shape of the interference pattern with filters in place. Two interference curves are shown in Fig. 6(a). The solid curve shows the interference pattern with no filters in place for a pump bandwidth of $3\Delta\nu_{\mathrm{cw}}$. For the dashed curve, a Gaussian filter function with width $\Delta\nu_{\mathrm{cw}}$ was introduced inside the integral in Eq. (15) and the calculation was repeated. As might be expected, the overall count rate is reduced, but the visibility increases from 0.205 to 0.721. The spectral filters have essentially blocked some of the distinguishable photon pairs. Spectral filters with a smaller bandpass will improve

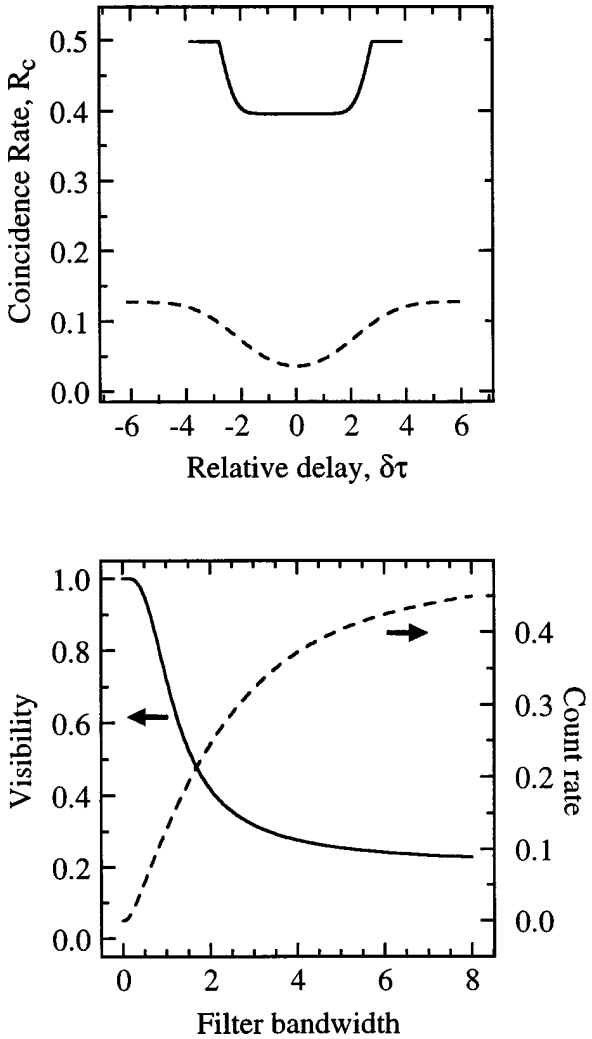

FIG. 6. (a) The coincidence rate plotted as a function of relative delay between the down-converted photons. The delay is normalized by $1/\Delta\nu_{\mathrm{cs}}$, the inverse of the characteristic bandwidth. The dashed curve corresponds to a spectral filter of width $\Delta\nu_{\mathrm{cw}}$ and the solid curve represents the pattern expected with no spectral filter in place. The pump bandwidth is $3\Delta\nu_{\mathrm{cw}}$. (b) Visibility of the interference pattern (left axis) and count rate (right axis) plotted as a function of filter bandwidth.

the visibility even further, but will result in a lower overall count rate. This can be seen in Fig. 6(b), which shows plots of visibility and count rate versus filter bandwidth. As the filter bandwidth increases, the visibility decreases while the count rate increases. This tradeoff can be managed by defining and optimizing a figure of merit. With a pump bandwidth of $3\Delta\nu_{cw}$, for example, the product of the count rate and the square of the visibility reaches maximum value with a filter bandwidth of $0.9\Delta\nu_{cw}$.

The calculations contained in this paper have been carried out for type-II down-conversion. It is interesting, though, to also consider type-I down-conversion when pumped by a broadband source. Because the two down-converted photons have the same polarization, the material dispersion has the same effect on each. The phase-matching function is therefore symmetric with respect to its two frequency arguments. As a result, the two photons would have identical spectra, although their energies would not be strictly anticorrelated. In addition, if the two photons were input into a Hong-Ou-Mandel interferometer, the visibility would not depend on the pump bandwidth.

IV. DISCUSSION

We have shown that the output of a type-II parametric down-converter pumped by a broadband source possesses characteristics not found in cw-pumped down-conversion. The state vector describing the output is a continuous superposition of two-photon states in which the probability amplitude for each state depends on the pump bandwidth, as well as the crystal parameters. The pump envelope function determines the range of pump energies available for down-conversion, and the phase-matching function determines how these energies are distributed to the two down-converted photons. Because the phase-matching function is not symmetric with respect to the two polarizations, the two down-converted photons are not exactly anticorrelated and their spectra are not identical. We have analyzed theoretically an experiment in which this reduced correlation plays an important role. We find that the visibility in fourth-order interference is reduced because of the additional information carried by the photons. The visibility can be restored, however, by placing spectral filters in front of the detectors.

The proposed experiment is similar to some of the quantum eraser experiments and proposals found in recent literature [21]. It is perhaps most similar to an experiment involving two photons produced in parametric down-conversion that interfere in a Hong-Ou-Mandel interferometer [22]. The photons are prepared so that they are orthogonally polarized before being mixed at the beam splitter and so no interference is observed in the coincidence count rate. By placing properly oriented polarizers before the detectors, the interference is restored. In both experiments, the visibility of the fourth-order interference is decreased by adding information to the system. The information is then ''erased'' after the photons are combined at a beam splitter, thus restoring the interference. There is an important distinction between the two experiments, though. In the polarization experiment, the relative phase between the two interfering paths may be adjusted by rotating the polarizers, making it possible to observe antifringes. The experiment described here does not possess an analogous feature.

Spontaneous parametric down-conversion pumped by a cw laser has proven to be a reliable and convenient source of correlated photons for the study of some of the more interesting features of quantum mechanics, but because the time of emission is completely random, cw-pumped down-conversion is inadequate for many of the recent experimental proposals involving states of three or more correlated photons. It is clear that independently pumped down-conversion crystals will not emit photons at nearly simultaneous times unless they are pumped with short optical pulses. The model presented in this paper shows that the photons emitted in this type of process are not, in general, as well correlated as those produced in cw-pumped down-conversion. This decreased correlation can have interesting consequences, as evidenced in the proposed experiment. A prudent choice of spectral filters for the down-converted photons can minimize the deleterious effects of the reduced correlation while retaining information about the emission time of the photons.

ACKNOWLEDGMENTS

This work was supported by the National Science Foundation (PHY-9512680). W.P.G. acknowledges financial support from the Laboratory for Laser Energetics.

[1] C. K. Hong, Z. Y. Ou, and L. Mandel, Phys. Rev. Lett. **59**, 2044 (1987).
[2] Z. Y. Ou and L. Mandel, Phys. Rev. Lett. **61**, 50 (1988).
[3] P. G. Kwiat, A. M. Steinberg, and R. Y. Chiao, Phys. Rev. A **47**, R2472 (1993).
[4] T. E. Kiess *et al.*, Phys. Rev. Lett. **71**, 3893 (1993).
[5] A. M. Steinberg, P. G. Kwiat, and R. Y. Chiao, Phys. Rev. Lett. **68**, 2421 (1992).
[6] A. V. Sergienko, Y. H. Shih, and M. H. Rubin, J. Opt. Soc. Am. B **12**, 859 (1995).
[7] A. Joobeur, B. E. A. Saleh, and M. C. Teich, Phys. Rev. A **50**, 3349 (1994).
[8] T. B. Pittman *et al.*, Phys. Rev. A **53**, 2804 (1996).
[9] B. Yurke and D. Stoler, Phys. Rev. A **46**, 2229 (1992).
[10] M. Zukowski *et al.*, Phys. Rev. Lett. **71**, 4287 (1993).
[11] M. Pavicic, Phys. Rev. Lett. **73**, 3191 (1994).
[12] D. M. Greenberger, M. Horne, and A. Zeilinger, in *Bell's Theorem, Quantum Theory, and Conceptions of the Universe*, edited by M. Kafatos (Kluwer, Dordrecht, 1989); D. M. Greenberger, Am. J. Phys. **58**, 1131 (1990).
[13] B. Yurke and D. Stoler, Phys. Rev. Lett. **68**, 1251 (1992).
[14] Y. H. Shih and M. H. Rubin, Phys. Rev. Lett. **182**, 16 (1993).
[15] T. B. Pittman, Phys. Lett. A **204**, 193 (1995).
[16] We take this expression to represent a single pulse in the pump field. In any real experimental situation, however, the pump will consist not of a single pulse, but a sequence of similar

pulses. In this case, calculated probabilities must be averaged over the ensemble of pulses. For a coherent pulse train, in which the amplitude and phase do not vary from pulse to pulse, this average leaves the results unchanged. If there are amplitude or phase fluctuations, the results are rendered correct by the inclusion of the ensemble average.

[17] J. G. Rarity, in *Fundamental Problems in Quantum Theory*, edited by D. M. Greenberger and A. Zeilinger (New York Academy of Sciences, Baltimore, MD, 1994), Vol. 755, p. 624.

[18] Z. Y. Ou, L. J. Wang, and L. Mandel, Phys. Rev. A **40**, 1428 (1989).

[19] Y. H. Shih *et al.*, Phys. Rev. A **50**, 23 (1994).

[20] Y. H. Shih and A. V. Sergienko, Phys. Rev. A **50**, 2564 (1994).

[21] P. G. Kwiat, A. M. Steinberg, and R. Y. Chiao, Phys. Rev. A **49**, 61 (1994).

[22] P. G. Kwiat, A. M. Steinberg, and R. Y. Chiao, Phys. Rev. A **45**, 7729 (1992).